Modeling and Measurements of Scattering from Road Surfaces at Millimeter-Wave Frequencies

Kamal Sarabandi, *Senior Member, IEEE*, Eric S. Li, and Adib Nashashibi, *Member, IEEE*

***Abstract*—Millimeter-wave radar-based sensors are being considered for a number of automotive applications including obstacle detection and collision warning, true-speed, and road-surface recognition. In this paper, the interaction of electromagnetic waves with asphalt road surfaces, possibly covered with ice or water, at millimeter-wave frequencies is studied. First, an experimental procedure for determining the effective dielectric constant of bituminous mixtures used in road-surface constructions is developed. In this procedure, the effective dielectric constant is derived using a simple inverse-scattering algorithm to the measured radar cross sections of cylindrical specimen of a standard asphalt mixture. Then the vector radiative transfer equation is used to formulate the scattering from a multilayer medium representing an ice- or water-covered asphalt surface. The University of Michigan polarimetric 94-GHz radar system was deployed for characterizing the polarimetric backscatter responses of asphalt surfaces under many physical conditions near grazing incidence angles (70°–88°). The measured backscatter coefficients and parameters of copolarized phase difference statistics of a dry asphalt surface with smooth interface at one incidence angle were used to derive the phase and extinction matrices of the asphalt medium. The experimentally determined phase and extinction matrices are substituted in the radiative transfer formulation to predict the scattering from asphalt surfaces under all conditions. Excellent agreement between theoretical predictions and measured quantities is obtained.**

***Index Terms*— Electromagnetic scattering, millimeter-wave measurements.**

I. Introduction

According to the National Highway Traffic Safety Administration, traffic accidents are among the leading causes of death in industrial countries. A study has shown that 90% of rear-end and 60% of head-on collisions can be prevented, provided that the drivers had been given one extra second of warning [1]. Advanced sensors that alert drivers to the potential hazards such as objects on the road or slippery surfaces can drastically reduce traffic accidents. Radars, when compared with optical and infrared sensors, offer two major advantages: 1) their operation is not hampered with inclement weather and 2) they provide the range and speed of targets directly. With advances in millimeter-wave (MMW) technology, millimeter-wave radar-based sensors for automotive applications have become economically viable. These applications include collision warning, intelligent cruise control, traction control, lane-change aid, etc. [2], [3]. In recent years, considerable efforts by many automobile industries and government agencies have been devoted toward the development of these MMW sensors. However, due to the lack of accurate knowledge of the radar backscatter behavior of targets and clutter in highway environment, the initial optimism has not yet led to a system that can perform properly, even with the most lax false-alarm rate requirement.

In this paper, as a first step, the theoretical and experimental aspects of electromagnetic wave scattering from asphalt surfaces are considered. Noting that in many radar applications detection and discrimination of a target in the presence of clutter can be enhanced significantly by appropriately choosing the optimal set of transmit and receive polarizations, the scattering responses of asphalt surfaces must be characterized polarimetrically. In a recent paper, it was shown that the *a priori* knowledge of the polarimetric responses of a number of distributed targets can be used to design an optimum nonpolarimetric radar for classifying the targets [4]. The number of influential physical parameters on radar responses of asphalt surfaces such as surface roughness, surface wetness, density, surface cover, etc. is rather large, which makes the effort of generating a comprehensive data set extremely difficult if not impossible. From a theoretical point of view, the problem at hand can be regarded as obtaining the solution for backscatter from a multilayer dense random medium. At millimeter-wave frequencies where the sizes of inhomogeneities in dense random medium are comparable to the wavelength, it is not always possible to theoretically determine an accurate description of random medium parameters such as extinction and phase matrices or the pair-distribution function. The method pursued in this paper makes use of experimental procedures to characterize the fundamental medium parameters needed in the vector radiative transfer formulation.

In what follows, first an experimental procedure for characterizing the effective dielectric constant of asphalt mixtures is developed. The effective dielectric constant is needed for determining the diffraction, propagation constant, and extinction coefficient of the mean field in dense asphalt mixtures. Next, the problem of volume scattering from a multilayer medium is formulated using the vector radiative transfer. Explicit expressions for backscattering coefficients and parameters of phase difference statistics are obtained in terms of elements of the phase and extinction matrices of the medium. In Section IV, experimental polarimetric backscatter data from asphalt surfaces under different physical conditions

Manuscript received March 19, 1997; revised July 8, 1997. This work was supported by the National Automotive Highway Systems Consortium (NAHSC) and U.S. Army Tank Automotive Command.

The authors are with the Radiation Laboratory, Department of Electrical Engineering and Computer Science, The University of Michigan, Ann Arbor, MI 48109 USA.

Publisher Item Identifier S 0018-926X(97)07993-3.

TABLE I
PARTICLE SIZE DISTRIBUTION OF ASPHALT SPECIMENS

Sieve Size in cm	% Passing
1.27	100
0.95	92
0.64	75
0.32	62
0.25	55
0.16	44
0.06	20
0.03	7
0.01	4.5

are presented and compared with the theoretical predictions.

II. EFFECTIVE DIELECTRIC CONSTANT OF ASPHALT

Asphalt can be considered as a composite material comprised of pebbles, sand, bitumen (asphalt), and air voids arranged in a random fashion. Electromagnetic scattering and propagation in a random medium are mostly influenced by the contrast in the complex permittivities and sizes (relative to the wavelength) of the constituent particles. Size distribution of rocks in asphalt mixtures may vary depending on the application [5]. Table I shows a typical particle-size distribution in an asphalt mixture used for construction of road surfaces. The pebbles, crushed rocks, and sand constitute 85–90% of the mixture and the rest is occupied by bitumen (5–7%) and air voids (5–8%). Except certain deleterious rocks such as clay stone or iron stone, the rocks in the asphalt mixture are arbitrary and are chosen according to the availability [6]. Due to the high-volume fraction of rocks and sand in asphalt mixtures, the effective dielectric constant is mostly influenced by the complex permittivities of rocks and sand particles. At low frequencies where the sizes of constituent particles are much smaller than the wavelength, the effective dielectric constant of the mixtures can be obtained from the dielectric constants and volume fraction of constituent particles using dielectric mixing formula such as Polder–Van Santen [7]. However, at high frequencies where the sizes of particles are comparable or larger than the wavelength, significant scattering in the medium occurs. This, in effect, increases the imaginary part of the effective dielectric constant. Recent experimental and numerical analysis have shown that simple low-frequency mixing formula can accurately predict the real part of the effective dielectric constants of random media at high frequencies [8], [9].

The literature concerning the dielectric properties of constituent components of asphalt mixtures at W-band frequencies is rather rare. The complex permittivities of different rocks are reported at 450 MHz and 35 GHz by Campbell and Ulrichs [10]. It is shown that the real part of the relative dielectric constants of rocks varies within the range 3–8 with a weak dependency on frequency. It is also shown that loss tangent for most rocks is relatively low. Bitumen, like rocks, is a nonpolar substance and its dielectric constant is expected to be a gentle function of frequency. Therefore, the real part of the effective dielectric constant of asphalt mixtures should be almost a constant as a function of frequency. As mentioned earlier, this generalization does not apply to the imaginary part of the mixture dielectric constant due to the presence of strong scatterers in the medium. Evaluation of the imaginary part of the effective dielectric constant or equivalently the extinction coefficient of a dense random medium is not very straight forward. The most advanced method, known as quasi-crystalline approximation (QCA) [11], [12], that takes multiple scattering among particles into account has been validated for single-particle type media with volume fractions less than 20%. Besides the shape and particle-size distributions, QCA requires the knowledge of the pair-distribution function of the particles in the medium which is very difficult to characterize.

Since the theoretical calculation of the effective dielectric constant of asphalt mixtures is not easy, we resorted to experimental procedures. As mentioned earlier, it is expected that the real part of effective permittivity of asphalt mixtures be almost independent of frequency and, therefore, a dielectric measurement at microwave frequencies should reveal the real part of the effective dielectric constant. The loss tangents of bitumen and rocks at microwave frequencies are rather low, which permits the dielectric characterization using a microwave resonator. Since the measurements should be accomplished nondestructively, a partially filled transmission-line-type resonator is most appropriate for this task. For this purpose we used a microstrip ring resonator at L-band frequencies. The resonant frequency of a ring resonator is inversely proportional to the perimeter of the ring and the square root of the effective dielectric constant of the microstrip substrate and the unknown medium. The choice of frequency determines the dimension of the ring resonator whose geometry is shown in Fig. 1. It is important that the dimension of the ring resonator be much larger than a typical dimension of the constituent particles of the mixture. This requirement ensures that the variability in the shift in resonant frequency as a function of resonator position is relatively small. Following the procedure outlined in [13], the dielectric constants of 15 smooth asphalt samples were measured using the L-band microstrip ring resonator. The real part of the effective dielectric constant of the asphalt mixtures at 1.1 GHz was found to be 3.33 ± 0.12.

To directly evaluate the effective dielectric constant of the asphalt mixtures at 94 GHz, a free-space measurement method was devised. In this approach cylindrical samples of an asphalt mixture with bitumen content 6.2% and air void content of 3.5% prepared by Midwest Testing Laboratories were measured. The particle size distribution of these specimens is reported in Table I. The desired density of the asphalt mixture is achieved using the Marshall method ASTM D1559 [14]. The cylindrical samples were constructed having three different heights—1.59, 2.38, and 6.35 cm—all having the same diameter of 10 cm. For each specified height, three specimen were made for verification of measurement consistency. The University of Michigan 94-GHz scatterometer system was used to measure the radar cross sections (RCS's) of the cylindrical samples. The cylindrical samples were positioned along the radar boresight with their circular base facing the

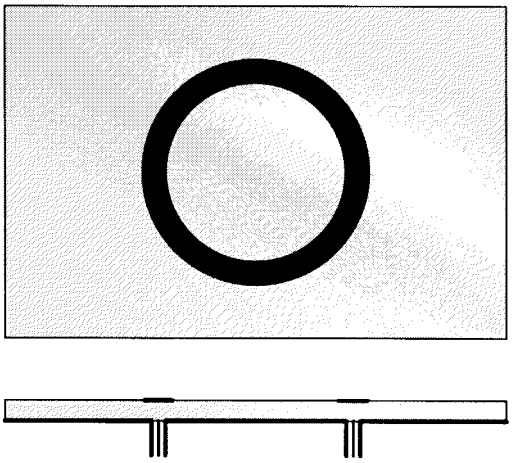

Fig. 1. Geometry of a ring resonator.

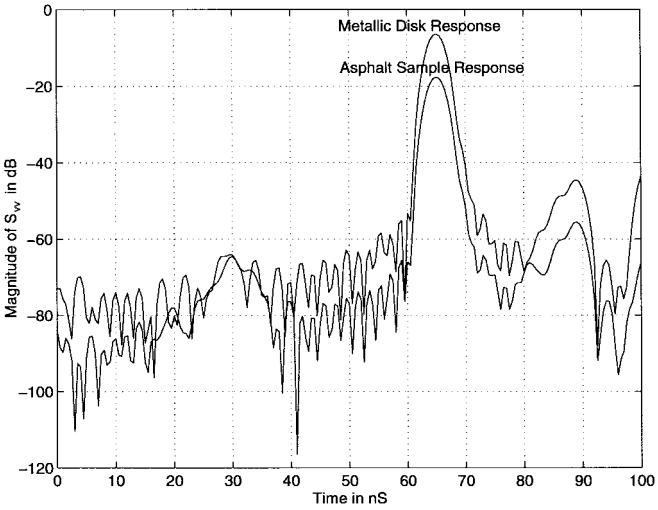

Fig. 2. The time-domain radar backscatter responses of a typical asphalt sample and the circular metallic disk.

radar and being perpendicular to the radar boresight direction. An accurate elevation-over-azimuth positioner was used to facilitate the positioning of the samples. First, a thick sample (6.35 cm) was placed in front of the radar and its backscatter was measured twice: sample alone and the sample backed by a circular metallic plate with diameter equal to that of the cylinder (10 cm). No change was observed in the measured RCS of the cylindrical sample once the metallic plate was attached. From this experiment it was concluded that the extinction in the asphalt medium is so high that the signal reflected off the metallic plate does not significantly contribute to the overall backscatter. In other words, the scattered field, in this case, originates from the lit surface of the cylinder only. Since the dimensions of the target (cylinder) is much larger than the wavelength ($\lambda = 3.19$ mm), physical optics approximation can be used to evaluate the RCS. According to this approximation the RCS of this target can be obtained from [16]

$$\sigma_c = \frac{4\pi A^2}{\lambda^2}|\Gamma_\circ|^2$$

where A is the surface area of the cylinder base, λ is the wavelength, and $\Gamma_\circ$ is the Fresnel reflection coefficient at normal incidence. Asphalt surface reflectivity was measured directly by comparing the backscatter of the metallic disk to that of the cylindrical sample at the same distance from the radar. Statistics of the surface reflectivity was obtained using all three samples and by measuring both the front and back of the samples. Fig. 2 shows the time-domain radar backscatter responses of a typical asphalt sample and the circular metallic disk. From about six independent backscatter measurements the surface reflectivity was calculated to be -11 ± 0.1 dB. Since the asphalt mixture is a low-loss material, the surface reflectivity is mostly dominated by the real part of the effective dielectric constant, hence

$$\epsilon_e' = \left(\frac{1+\Gamma_\circ}{1-\Gamma_\circ}\right)^2. \tag{1}$$

Using the measured reflectivity in (1), the real part of the effective dielectric constant of the asphalt mixtures at 94 GHz is found to be $\epsilon_e' = 3.18 \pm 0.04$. This measurement is consistent with the low-frequency measurement conducted at L-band.

Next, we attempted to evaluate the imaginary part of the effective dielectric constant using the thiner samples. RCS's of cylindrical samples with height 2.38 cm were measured and, as before, no change in the measured RCS's was observed when the metallic circular disk was placed behind the cylindrical samples. This indicates that the two-way attenuation is still too high (note that the power transmissivity at the interface between air and asphalt is more than 92%). Similar experiments were conducted using the thinnest samples (1.59 cm). For these samples the change in RCS with and without the metallic disk was of the order of only 0.1 dB. Obviously the change in the RCS is not high enough to allow for an accurate characterization of the imaginary part of the effective dielectric constant, however, an approximate estimate can be obtained. The reflection coefficient of a metal-backed layer of thickness d at normal incidence is given by

$$\Gamma_m = \frac{\Gamma_\circ - e^{2ik_a d}}{1 - \Gamma_\circ e^{2ik_a d}} \tag{2}$$

where $k_a = \beta + i\alpha$ is the complex propagation constant in the asphalt mixture. Using (2), the attenuation constant and the imaginary part of the effective dielectric constant of the asphalt mixture at 94 GHz are, respectively, found to be $\alpha \approx 54$ Np/m and $\epsilon_e'' \approx 0.1$. Note that although a thinner asphalt sample exhibits a higher difference between RCS's of the sample with and without the metallic disk, the calculation of ϵ_e'' would still not be accurate for two reasons: 1) the diameters of about 10% of particles in the asphalt mixture are larger than 1 cm, which limits the thickness of the cylindrical samples and 2) the sample has to be many wavelengths long to allow for the interaction of the electromagnetic wave with the random medium.

III. Theoretical Analysis

In this section, the problem of scattering from an asphalt surface possibly covered with a thin layer of ice or water

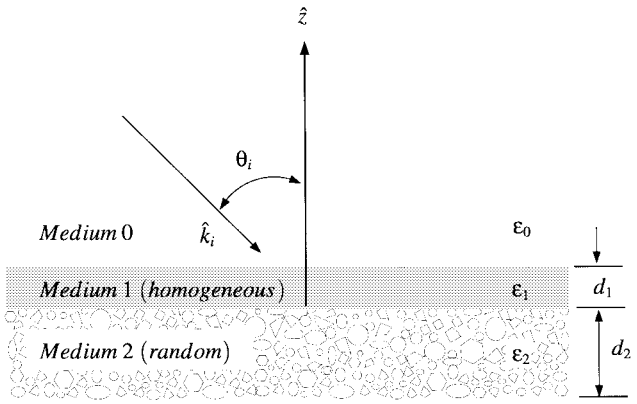

Fig. 3. The geometry of the scattering from an asphalt surface possibly covered with a thin layer of ice or water.

is considered. The geometry of the scattering problem is shown in Fig. 3 where the ice or water layer is considered as a homogeneous layer with thickness d_1. The asphalt is modeled as a layer of dense random medium with thickness d_2 and on top of a relatively smooth gravel surface. Suppose a uniform plane wave in air (medium 0) is incident on the multilayer medium. At the interface, the incident ray refracts and enters the random medium where scattering in all directions (including the backscatter direction) takes place. Interaction of electromagnetic waves with random media can be explained using a heuristic approach known as radiative transfer (RT) method. The formulation of RT is based on conservation of energy and has been successfully applied to many remote sensing problems [18]–[20]. In this theory, the polarimetric flow of electromagnetic energy through a random medium can be explained from the solution of a vector integrodifferential equation given by

$$\frac{\boldsymbol{I}(\hat{s},\boldsymbol{r})}{ds} = -\boldsymbol{\kappa}\boldsymbol{I}(\hat{s},\boldsymbol{r}) + \iint_{4\pi} \boldsymbol{P}(\hat{s},\hat{s}')\boldsymbol{I}(\hat{s}',\boldsymbol{r})\, d\Omega' \qquad (3)$$

where $\boldsymbol{I}$ is an unknown 4×1 vector specific intensity (power density per unit solid angle), $\boldsymbol{\kappa}$ is the 4×4 extinction matrix and $\boldsymbol{P}$ is the 4×4 phase matrix. The extinction matrix characterizes the attenuation of the vector specific intensity due to absorption and scattering. The phase matrix relates the average specific intensity scattered by a unit volume of the random media into direction $\hat{s}$ to the incident intensity upon the unit volume from the direction $\hat{s}'$.

For an elliptically polarized monochromatic plane wave the incident specific intensity $\boldsymbol{I}^i$ is defined through the modified Stokes parameters I_v, I_h, U, and V as follows:

$$\boldsymbol{I}^i = \begin{bmatrix} I_v \\ I_h \\ U \\ V \end{bmatrix} = \frac{1}{\eta_o} \begin{bmatrix} |E_v|^2 \\ |E_h|^2 \\ 2\,\mathrm{Re}(E_v E_h^*) \\ 2\,\mathrm{Im}(E_v E_h^*) \end{bmatrix} \qquad (4)$$

where η_o is the intrinsic impedance of free-space. Note that the scattered field from a distributed target is a spherical wave. The vector specific intensity is also defined in terms of Stokes parameters, but the definition includes normalization by the solid angle $A\cos\theta_s/r^2$ where A is the illumination area, r is the distance between the distributed target and the observation point, and θ_s is the angle between the outward normal to A and the vector defining the direction from the target to the observation point. Hence, the scattered intensity from a random medium is defined as

$$\boldsymbol{I}^s = \begin{bmatrix} I_v^s \\ I_h^s \\ U^s \\ V^s \end{bmatrix} = \frac{r^2}{\eta_o A\cos\theta_s} \begin{bmatrix} \langle |E_v^s|^2 \rangle \\ \langle |E_h^s|^2 \rangle \\ 2\,\mathrm{Re}(\langle E_v^s E_h^{s*} \rangle) \\ 2\,\mathrm{Im}(\langle E_v^s E_h^{s*} \rangle) \end{bmatrix} \qquad (5)$$

where $\langle\ \rangle$ denotes ensemble average. The bistatic scattering coefficient $\sigma^\circ_{\alpha\beta}$ corresponding to a β-polarized incident plane wave giving rise to α-polarized spherical wave can be obtained from [12]

$$\sigma^\circ_{\alpha\beta}(\pi-\theta_0,\phi_0;\theta_s,\phi_s) = \frac{4\pi\cos\theta_s I^s_\alpha(\theta_s,\phi_s)}{I^i_\beta(\pi-\theta_0,\phi_0)} \qquad (6)$$

where $(\pi-\theta_0,\phi_0)$ denotes the direction of the downward-going incident intensity and (θ_s,ϕ_s) denotes the direction of the upward-going scattered intensity. We note that $\theta_s = \theta_0$ and $\phi_s = \pi + \phi_0$ corresponds to scattering in the backward direction.

The phase and extinction matrices are the fundamental quantities in the RT model. That is, if these quantities could be specified, then, indeed, the medium is completely characterized and scattering for any arbitrary configuration could be predicted provided that the boundary conditions are accounted for appropriately. As mentioned earlier, asphalt mixture is a complex medium for electromagnetic waves where even most advanced theoretical methods, such as dense medium radiative transfer model [17], are inadequate to correctly predict the phase and extinction matrices. To circumvent this problem, a modeling effort based on partly radiative transfer and partly experimental analysis is proposed. In the proposed technique, unlike the standard methods, we do not attempt to derive the form of the phase and extinction matrices in terms of particle size, shape, density, and permittivity. Instead, we propose to invert for them directly, from *controlled* polarimetric backscatter radar measurements. The scattering elements in the medium are considered as clusters to underscore the point that we are considering "effective" particles in this treatment that may consist of correlated groups of individual physical particles and/or multiple scattering effects. To simplify the problem further, we assume that a first-order model can be used to comprehend the scattering. This assumption stems from the fact that the far-field scattering albedo (excluding near-field particle interactions) in an asphalt medium is relatively small.

The standard practice in solving the RT equation iteratively is to split the intensity vector into upward-going $(\boldsymbol{I}^+(\theta,\phi,z))$ and downward-going $(\boldsymbol{I}^-(\theta,\phi,z))$ components, noting that $0<\theta<\pi/2$. The first-order solution of RT equation has been reported in the literature [12], [23], and [24] and will not be repeated here. The appropriate boundary conditions for the problem at hand are as follows. In practice, the layer thickness of most asphalt surfaces exceeds 5 cm. In the previous section, it was shown that the attenuation constant of the mean field in asphalt mixtures exceeds 54 Np/m at 94 GHz. Hence, a 5-cm layer of asphalt appears as a semi-infinite medium for electromagnetic waves at W-band frequencies. This property

simplifies the boundary condition at the top interface of the asphalt layer. The downward-going intensity just below the interface in medium 2 is related to the incident intensity above the interface between medium 0 and medium 1 and is given by

$$\boldsymbol{I}^{-}(\pi-\theta,\phi,0^{-})=\boldsymbol{T}_{02}\boldsymbol{I}^{i}(\pi-\theta_0,\phi_0,d_1^{+})\delta(\theta-\theta_2)\delta(\phi-\phi_0) \tag{7}$$

where θ_2 denotes the angle of propagation of the mean-field in medium 2 calculated from the Fresnel law of refraction and $\boldsymbol{T}_{02}$ is the transmissivity matrix. The boundary condition that relates the scattered upward-going intensity in medium 2 just below the surface to the upward-going intensity in medium 0 is simply given by

$$\boldsymbol{I}^{s}(\theta_0^{s},\phi_0^{s},d_1^{+})=\boldsymbol{T}_{20}\boldsymbol{I}^{+}(\theta_2^{s},\phi_0^{s},0^{-}). \tag{8}$$

For intensity vectors constructed from Stokes parameters the transmissivity matrix can be calculated from

$$\boldsymbol{T}_{02}=\frac{n_2^2\eta_0\cos\theta_2}{n_0^2\eta_2\cos\theta_0}\cdot\begin{bmatrix}|t_{02}^{v}|^2 & 0 & 0 & 0\\ 0 & |t_{02}^{h}|^2 & 0 & 0\\ 0 & 0 & \mathrm{Re}(t_{02}^{v}t_{02}^{h*}) & -\mathrm{Im}(t_{02}^{v}t_{02}^{h*})\\ 0 & 0 & \mathrm{Im}(t_{02}^{v}t_{02}^{h*}) & \mathrm{Re}(t_{02}^{v}t_{02}^{h*})\end{bmatrix} \tag{9}$$

where n_j and η_j are the index of refraction and intrinsic impedance of medium j, respectively. Also, t_{02}^{v} and t_{02}^{h} are the v-polarized and h-polarized field-transmission coefficients from medium 0 to medium 2. Equation (9) can be used for the calculation of $\boldsymbol{T}_{20}$ by simply interchanging the subscripts 0 and 2.

Plane wave field-transmission coefficient in layered media can be obtained following the procedure outlined in [26]. For the three-layered problem the h-polarized field-transmission coefficient is given by

$$t_{02}^{h}=e^{ik_{1z}d_1}\frac{(1+r_{12}^{h})(1+r_{01}^{h})}{1+r_{01}^{h}r_{12}^{h}e^{i2k_{1z}d_1}} \tag{10}$$

where r_{pq}^{h} $(p\in 0,1,q\in 1,2)$ is Fresnel reflection coefficient at the interface of medium p and medium q and is given by

$$r_{pq}^{h}=\frac{k_{pz}-k_{qz}}{k_{pz}+k_{qz}}.$$

Here, k_{pz} is the z component of propagation constant in medium p, which can be calculated from

$$k_{pz}=k_0\sqrt{\epsilon_p-\sin^2\theta_0}.$$

The v-polarized field-transmission coefficient can be obtained from (10) by multiplying the right-hand-side by η_2/η_0 and replacing r_{pq}^{h} with r_{pq}^{v} given by

$$r_{pq}^{v}=\frac{\epsilon_q k_{pz}-\epsilon_p k_{qz}}{\epsilon_q k_{pz}+\epsilon_p k_{qz}}.$$

Iterative solution of RT equation subject to the aforementioned boundary equations up to the first order results in the following simple expression for the backscattered intensity:

$$\boldsymbol{I}^{s}(\theta_0,\phi_0+\pi,d_1^{+})=\boldsymbol{T}_{20}\boldsymbol{A}\boldsymbol{T}_{02}\boldsymbol{I}^{i}(\pi-\theta_0,\phi_0,d_1^{+}). \tag{11}$$

In (11), $\boldsymbol{A}$ is a 4×4 matrix whose elements are given by

$$[\boldsymbol{A}]_{ij}=\frac{1}{\lambda_i+\lambda_j}\cdot[\boldsymbol{Q}^{-1}\boldsymbol{P}\boldsymbol{Q}]_{ij}$$

where λ_i and $\boldsymbol{Q}$ are the ith eigenvalue and the matrix of eigenvectors of the extinction matrix, respectively. Note that particle arrangement in asphalt mixtures is statistically homogeneous and symmetrical. That is, there is no preferred orientation for the constituent particles in the medium (isotropic random medium). In this case, it is expected that the extinction matrix be reduced to a scalar quantity (κ), which will further simplify (11) to

$$\boldsymbol{I}^{s}(\theta_0,\phi_0+\pi,d_1^{+})=\frac{1}{2\kappa}\boldsymbol{T}_{20}\boldsymbol{P}\boldsymbol{T}_{02}\boldsymbol{I}^{i}(\pi-\theta_0,\phi_0,d_1^{+}). \tag{12}$$

It is also shown that for isotropic random media, the phase matrix in backscatter direction can be expressed in terms of only four independent parameters [25]

$$\boldsymbol{P}=\begin{bmatrix}p_1 & p_2 & 0 & 0\\ p_2 & p_1 & 0 & 0\\ 0 & 0 & p_3+p_2 & -p_4\\ 0 & 0 & p_4 & p_3-p_2\end{bmatrix}. \tag{13}$$

The zero entries in (13) are a result of lack of correlation between copolarized and cross-polarized components of the scattering matrix per unit volume of the random medium. Using (12) and (13) in (6), the following simple expressions for the backscattering coefficients are obtained:

$$\begin{aligned}\sigma_{vv}^{\circ}&=4\pi\cos\theta_0|t_{02}^{v}|^2|t_{20}^{v}|^2\frac{p_1}{2\kappa}\\ \sigma_{hh}^{\circ}&=4\pi\cos\theta_0|t_{02}^{h}|^2|t_{20}^{h}|^2\frac{p_1}{2\kappa}\\ \sigma_{vh}^{\circ}&=4\pi\cos\theta_0|t_{02}^{h}|^2|t_{20}^{v}|^2\frac{p_2}{2\kappa}\\ \sigma_{hv}^{\circ}&=4\pi\cos\theta_0|t_{02}^{v}|^2|t_{20}^{h}|^2\frac{p_2}{2\kappa}.\end{aligned} \tag{14}$$

Besides the backscattering coefficients, the phase difference between the copolarized backscattered components contains information about the target as well. The statistics of the phase difference can be obtained from the Mueller matrix [15]. The probability density function of the phase difference $(\phi_{vv}-\phi_{hh})$ is characterized in terms of two scalar parameters known as the degree of correlation (α) and the mean-phase difference (ζ). Recognizing the product $(1/2\kappa)\boldsymbol{T}_{20}\boldsymbol{P}\boldsymbol{T}_{02}$ in (12) as the Mueller matrix $(\boldsymbol{M})$, the degree of correlation and the mean-phase difference can be, respectively, computed from

$$\alpha=\frac{1}{2}\sqrt{\frac{(M_{33}+M_{44})^2+(M_{34}-M_{43})^2}{M_{11}M_{22}}} \tag{15}$$

$$\zeta=\tan^{-1}\left(\frac{M_{43}-M_{34}}{M_{33}+M_{44}}\right). \tag{16}$$

After some algebraic manipulations, it can be shown that

$$\begin{aligned}M_{33}+M_{44}&=\{\mathrm{Re}[Z_1Z_2]p_3-\mathrm{Im}[Z_1Z_2]p_4\}/\kappa\\ M_{43}-M_{34}&=\{\mathrm{Im}[Z_1Z_2]p_3+\mathrm{Re}[Z_1Z_2]p_4\}/\kappa\end{aligned} \tag{17}$$

where $Z_1=t_{20}^{v}t_{20}^{h*}$ and $Z_2=t_{02}^{v}t_{02}^{h*}$. Using the above equations in (15) and noting that $M_{11}=|t_{02}^{v}|^2|t_{20}^{v}|^2(p_1/2\kappa)$

and $M_{22} = |t_{02}^h|^2 |t_{20}^h|^2 (p_1/2\kappa)$, it can easily be shown that

$$\alpha = \sqrt{\frac{p_3^2 + p_4^2}{p_1^2}}. \tag{18}$$

It is interesting to note that the above expression for the degree of correlation is the same as the *intrinsic* degree of correlation of the medium (α_i) obtained from the medium phase function. That is the planar interface between a multilayer homogeneous medium and the random medium does not affect the degree of correlation between the vertical and horizontal backscattered signals. Similarly, defining the intrinsic mean phase difference of the medium by

$$\zeta_i = \tan^{-1} \frac{p_4}{p_3}$$

the mean phase difference given by (16) can be simplified to

$$\zeta = \zeta_i + \zeta_t \tag{19}$$

where ζ_t is defined as the total transition phase difference given by

$$\zeta_t = \angle(t_{20}^v t_{20}^{h*}) + \angle(t_{02}^v t_{02}^{h*}).$$

As expected, the mean-phase difference is the sum of the mean-phase difference caused by the random media and the phase difference introduced by the interface.

IV. Experimental Results

In the previous section, the mathematical framework for characterizing the millimeter-wave scattering responses of road surfaces possibly covered with a layer of ice or water was laid. It was shown that the backscattering coefficients and the statistics of the phase difference can be obtained from the four independent elements of the medium. In this section, polarimetric backscatter measurements at 94 GHz conducted on asphalt surfaces under a wide range of conditions are presented and compared with the theoretical results. In these experiments, the University of Michigan fully polarimetric 94-GHz radar system was used to collect the backscattering responses of the targets over the angular range 70°–88°. This radar is a stepped frequency radar capable of transmitting a linear chirped signal with a bandwidth of 2 GHz and can be operated in either coherent or coherent on receive modes [21]. Fig. 4 shows the major components of the radar system, which include: 1) the radar front-end; 2) a network analyzer; and 3) a computer. The radar front-end (RF unit) performs the up- and down-conversion of the network analyzer signal to the desired W-band frequency. The network analyzer (HP 8753C) is used as the IF transceiver of the system with two independent receive channels, which allows simultaneous reception of v- and h-polarized backscattered signals. A 486 processor-based computer is used to automate the measurements and store the data. The motion control card inside the computer together with dc motor amplifiers and optical encoders command and control the mechanical polarization switches and a two-dimensional radar gimbal assembly.

The gimbal assembly is a true elevation-over-azimuth positioner, which is used to scan the distributed targets (asphalt surfaces). In this study at least 80 spatial independent samples for each target at each incidence angle were collected to acquire the desired backscatter statistics. The measured data were calibrated using a metallic sphere according to the procedure outlined in [21]. The external calibration procedure removes the systematic errors (such as channel imbalances and antenna cross-talks) from the measured data.

Fig. 4. The University of Michigan 94-GHz fully polarimetric radar system.

Two measurement sites were considered for the intended experiments. At site 1, the asphalt surface was about a year old, having a relatively smooth interface. Backscatter measurements were conducted for three different conditions at this site: 1) dry asphalt surface; 2) wet asphalt surface with surface-water content 0.46 kg/m ^{2}; and 3) asphalt surface covered with a 1.4-mm-thick ice layer. Site 2 was chosen as the repeatability test site. The asphalt surface of this site, similar to site 1, was relatively new with smooth interface. The surface roughness of the asphalt layer was measured using a laser ranging system with a range resolution 0.1 mm. At each site a minimum of 10 linear traces of 40-cm-long surface profiles were collected with a horizontal resolution of 0.2 mm. It was found that the surface roughness statistics of sites 1 and 2 were very similar with rms height and surface correlation length of approximately 0.34 and 4.2 mm, respectively.

The theoretical formulation provided in the previous section only accounts for the volume scattering and totally ignores the contribution from the rough-surface scattering. The reflectivity and transmissivity of the coherent field (mean-field) at the rough interface between two homogeneous media are proportional to $e^{-k_0^2 \cos^2(\theta_0) s^2}$ where s is the root mean square (rms) height of the rough surface [22]. If this factor is close to unity, most of power remains in the coherent field and contribution from rough surface scattering is insignificant. This is the case for asphalt surfaces of sites 1 and 2. The measured backscatter data (backscattering coefficients and phase statistics) of dry asphalt from site 1 was used in (14), (18), and (19) to find the phase matrix elements and are tabulated in Table II. Fig. 5(a)–(c) shows the comparison between the measured and the theoretical prediction for the copolarized and cross-polarized backscattering coefficients of dry asphalt surfaces of sites 1 and 2. It is shown that the backscattering responses of the asphalt surfaces are independent of site location and that the agreement between the measurements and the theory

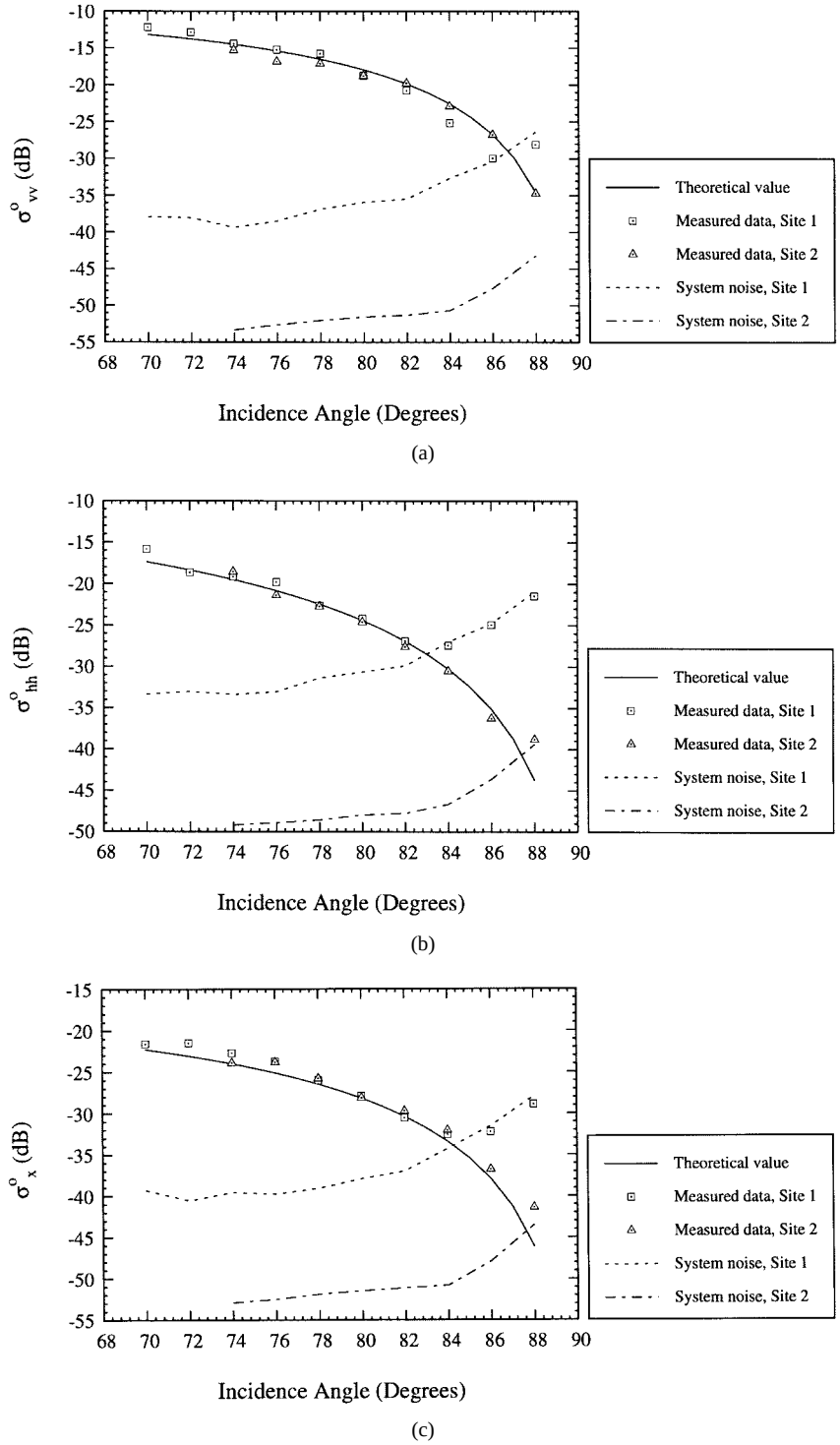

Fig. 5. The comparison between the measured data and the theoretical prediction for copolarized and cross-polarized backscattering coefficients of dry asphalt surfaces at sites 1 and 2.

is excellent over all angles of incidence. The dashed lines in these figures indicate the system noise-equivalent backscattering coefficients (noise floor). The system noise-equivalent backscattering coefficient for site 2 was improved using a coherent averaging technique during data collection.

As mentioned earlier, in site 1 polarimetric backscatter data were also collected from the asphalt surface covered with a thin layer of ice and water. Fig. 6 shows the copolarized and cross-polarized measured and calculated backscattering coefficients of ice-covered asphalt surface. In these calculations, the

TABLE II
NORMALIZED ELEMENTS OF PHASE MATRIX OF ASPHALT MEDIUM AT 94 GHz OBTAINED FROM THE POLARIMETRIC BACKSCATTER MEASUREMENTS OF SITE 1

p_1/κ	p_2/κ	p_3/κ	p_4/κ
2.36×10^{-2}	4.72×10^{-3}	1.16×10^{-2}	1.40×10^{-3}

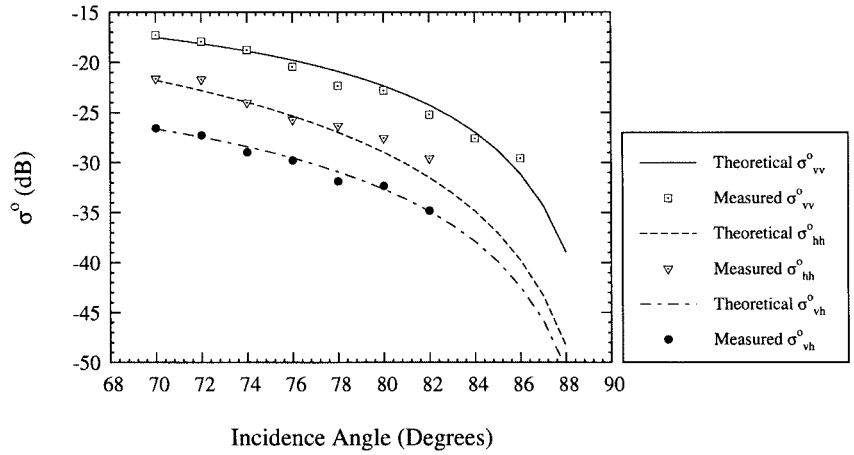

Fig. 6. The comparison between the measured data and the theoretical prediction for copolarized and cross-polarized backscattering coefficients of ice-covered asphalt surface of site 1.

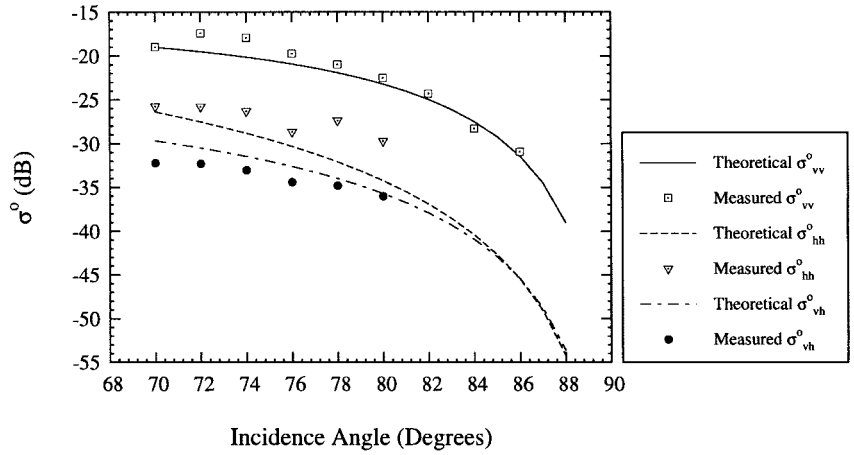

Fig. 7. The comparison between the measured data and the theoretical prediction for copolarized and cross-polarized backscattering coefficients of wet asphalt surface of site 1.

measured mean ice-layer thickness of 1.4 mm and fresh-water ice-dielectric constant of $\epsilon_i = 3.1 + i0.27$ [23] were used. As before, the agreement is excellent over the angular range where the measurements were not corrupted by the system noise. Fig. 7 shows the theoretical and measured backscattering coefficients of the wet asphalt surface. It is shown that the radar backscatter response drops significantly when the surface becomes wet. For the theoretical calculation in this case, the dielectric constant of water was calculated using Debye formulation given in [23]. It was found that the dielectric constant given by Debye formulation $(\epsilon_w = 5.6 + i7.8)$ provided an underestimation for the backscatter measurement. In this case, a thin film of water covered the asphalt surface (average thickness = 0.46 mm) where a significant fraction of the water molecules were bound to the surface. The dielectric constant of bound water is different from that of free water [23] and, therefore, the effective dielectric constant of a thin film of water is expected to be different as well. To characterize the effective dielectric constant of a thin film of water on an asphalt surface, the RCS's of the cylindrical asphalt samples were measured after a thin film of water was sprayed on their surfaces. The reflection coefficients of the wet asphalt surfaces were calculated from which the effective dielectric constant of thin water films was found to be $\epsilon_w = 5.6 + i1.7$. This value was used in the calculation of σ° and the results are shown in Fig. 7. As is shown by (18), the degree of correlation of asphalt surfaces should be independent of incidence angle and surface cover. Fig. 8 shows that the measured α's are indeed independent of incidence angle, however, there is some minor dependency on the surface-cover type which may be resulted from the surface roughness whose effect is not accounted for in this model. Data measured at lower grazing angles are excluded because of noise corruption. Fig. 9 shows the comparison between the calculated and measured mean phase difference (ζ). Average discrepancy of less than 10° is achieved.

V. Conclusion

Millimeter-wave polarimetric radar phenomenology of asphalt surfaces was investigated thoroughly. A scattering model based on the vector radiative transfer theory and experimental analysis was developed for predicting the radar backscattering responses of asphalt surfaces at 94 GHz. First, the effective dielectric constant of asphalt mixtures was obtained using

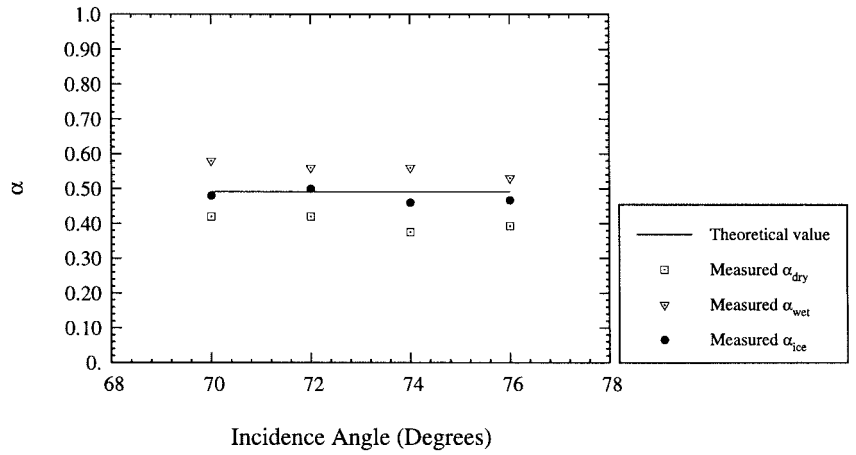

Fig. 8. The measured and calculated degree of correlation (α) of dry, wet, and ice-covered asphalt surfaces.

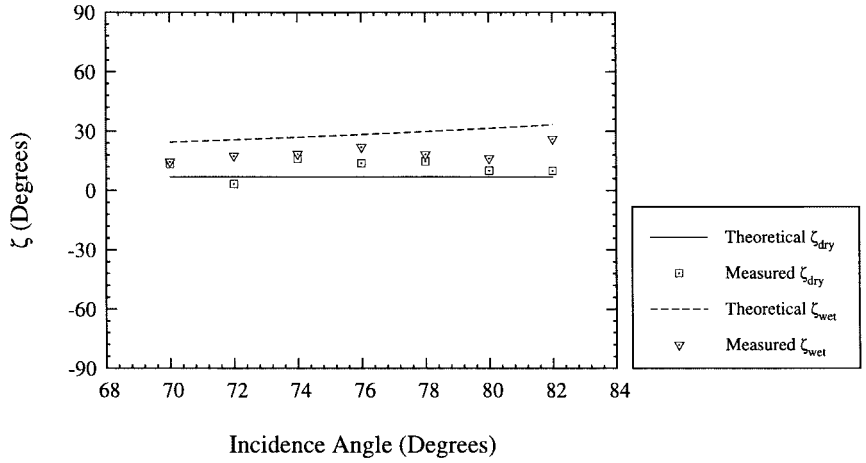

Fig. 9. The measured and calculated mean-phase difference (ζ) of dry and wet asphalt surfaces.

RCS measurements of cylindrical asphalt samples at normal incidence. The fundamental quantities of the RT model were obtained from a polarimetric backscatter measurement of a dry asphalt surface. These quantities were then used to predict the backscattering coefficients and phase-difference statistics of asphalt surfaces covered with water and ice over a wide range of incidence angles. The University of Michigan W-band polarimetric scatterometer system was used to collect the polarimetric backscattering responses of asphalt surfaces under many physical conditions. It was shown that the theoretical results and the measured quantities were in excellent agreement. Similar models can also be developed for other smooth road surfaces such as concrete.

REFERENCES

[1] K. Enke, *7th Int. Technol. Conf. Experimental Safety Veh.*, 1979.
[2] T. Rose, "Intelligent vehicle highway systems: Going places fast," *Microwave J.*, pp. 172–178, May 1993.
[3] L. Eriksson and S. Broden, "High performance automotive radar," *Microwave J.*, pp. 24–38, Oct. 1996.
[4] K. Sarabandi and E. S. Li, "Characterization of optimum polarization for multiple target discrimination using genetic algorithms," *IEEE Trans. Antennas Propagat.*, to be published.
[5] *1990 Standard Specifications For Construction*, Michigan Dept. Transportation, 1990, pp. 466–483.
[6] H. A. Wallace and J. R. Martin, *Asphalt Pavement Engineering.* New York: McGraw-Hill, 1967, pp. 43–62.
[7] D. Polder and J. H. Van Santen, "The effective permeability of mixtures of solids," *Phys.*, vol. 12, no. 5, pp. 1257–1271, Aug. 1946.
[8] K. Sarabandi and P. Siqueira, "Numerical scattering analysis for two dimensional dense random media: Characterization of effective permittivity," *IEEE Trans. Antennas Propagat.*, to be published.
[9] A. Nashashibi and K. Sarabandi, "Experimental characterization of the effective propagation constant of dense random media," *IEEE Trans. Antennas Propagat.*, to be published.
[10] M. J. Campbell and J. Ulrichs, "Electrical properties of rocks and their significance for lunar radar observations," *J. Geophys. Res.*, vol. 74, pp. 5867–5881, 1969.
[11] M. Lax, "Multiple scattering of waves—II: The effective field in dense systems," *Physical Rev.*, vol. 85, no. 4, pp. 621–629, Feb. 15, 1952.
[12] L. Tsang, J. Kong, and R. Shin, *Theory of Microwave Remote Sensing.* New York: Wiley, 1985.
[13] K. Sarabandi and E. S. Li, "A microstrip ring resonator for noninvasive dielectric measurements," *IEEE Trans. Geosci. Remote Sensing.*, vol. 35, pp. 1223–1231, Sept. 1997.
[14] *1996 Annual Book of ASTM Standards—Construction*, 1996, sect. 4, pp. 137–142.
[15] K. Sarabandi, "Derivation of phase statistics of distributed targets from the Mueller matrix," *Radio Sci.*, vol. 27, no. 5, pp 553–560, 1992.
[16] T. B. A. Senior and K. Sarabandi, "Scattering models for point targets," in *Radar Polarimetry for Geoscience Applications*, F.T. Ulaby and C. Elachi, Eds. Dedham, MA: Artech House, 1990.
[17] L. Tsang and A. Ishimaru, "Radiative wave equations for vector electromagnetic propagation in dense nontenuous media," *J. Electromagn. Waves Appl.*, vol. 1, no. 1, pp. 52–72, 1987.

[18] F. T. Ulaby, K. Sarabandi, K. McDonald, M. Whitt, and M. C. Dobson, "Michigan microwave canopy scattering model," *Int. J. Remote Sensing*, vol. 11, no. 7, pp. 1223–1253, July 1990.
[19] C. M. Lam and A. Ishimaru, "Calculation of Mueller matrices and polarization signatures for a slab of random medium using vector radiative transfer," *IEEE Trans. Antennas Propagat.*, vol. 41, pp. 851–862, July 1993.
[20] R. West, L. Tsang, and D. P. Winebrenner, "Dense medium radiative transfer theory for two scattering layers with a Rayleigh distribution of particle sizes," *IEEE Trans. Geosci. Remote Sensing.*, vol. 31, pp. 426–437, Mar. 1993.
[21] A. Nashashibi, K. Sarabandi, and F. T. Ulaby, "A calibration technique for polarimetric coherent-on-receive radar system," *IEEE Trans. Antennas Propagat.*, vol. 43, pp. 396–404, Apr. 1995.
[22] F. T. Ulaby, R. K. Moore, and A. K. Fung, *Microwave Remote Sensing—Vol. II*. Norwood, MA: Artech House, 1982, ch. 12, pp. 1006–1010.
[23] ———, *Microwave Remote Sensing—Vol. III*. Norwood, MA: Artech House, 1986, ch. 13, Appendixes E2–E3, pp. 2020–2028.
[24] K. Sarabandi, "Electromagnetic scattering from vegetation canopies," Ph.D. dissertation, Univ. Michigan, Ann Arbor, 1989.
[25] J. R. Kendra, "Microwave remote sensing of snow: An empirical/theoretical scattering model for dense random media," Ph.D. dissertation, Univ. Michigan, Ann Arbor, 1995.
[26] J. A. Kong, *Electromagnetic Wave Theory*. New York: Wiley, 1986, pp. 120–132.

Kamal Sarabandi (S'87–M'90–SM'92), for photograph and biography, see p. 867 of the May 1997 issue of this TRANSACTIONS.

Eric S. Li received the B.S. degree from Tamkang University, Taipei, Taiwan, in 1986, and the M.S. degree in electrical engineering from the State University of New York, Stony Brook, in 1987. He is currently working toward the Ph.D. degree in electrical engineering at the University of Michigan, Ann Arbor.

From 1988 to 1992 he worked as a Microwave Engineer in the cellular phone industry. His current research interests include polarimetric millimeter-wave radar systems, calibration and measurement technique, electromagnetic scattering, and millimeter-wave remote sensing.

Adib Nashashibi (S'82–M'95) received the B.Sc. and M.Sc. degrees in electrical engineering from Kuwait University, Kuwait, in 1985 and 1988, respectively, and the Ph.D. degree in electrical engineering from the University of Michigan, Ann Arbor, in 1995.

He is presently a Research Fellow at the Radiation Laboratory, University of Michigan. His research interests include microwave remote sensing, polarimetric millimeter-wave radars, calibration and measurement techniques, electromagnetic wave propagation, and scattering in random media.